

# Carrier Relaxation Dynamics in Self-Assembled Quantum Dots

Spectroscopic analysis group

Valentin G. Davydov, Ivan V. Ignatiev, and Igor E. Kozin

Carrier relaxation dynamics is studied by the technique of the electric field induced nonradiative losses and by the Photoluminescence kinetics measurements. Different channels of the carrier relaxation are observed for the heterostructures with InP and InGaAs quantum dots. The conditions when a phonon-assisted carrier relaxation occurs are determined. A few evidences of relatively fast acoustic-phonon-assisted relaxation are found. Different mechanisms of acceleration of the carrier relaxation via carrier-carrier scattering are discussed. Most important of them are an Auger-like process, an interaction with excess carrier in charged quantum dots and an electric-current-induced relaxation.

## I. INTRODUCTION

Carrier relaxation dynamics in quantum dots (QD's) attract much attention during the last decade because it is assumed to be significantly different from those in bulk material due to the discrete energy spectrum. Generally two main mechanisms of relaxation are considered. The first one is the phonon assisted relaxation when a hot carrier relaxes to its ground state with emission of one or few phonons. However, theoretical analysis predicts that relaxation with longitudinal optical (LO) phonon emission is possible only for a narrow energy window for the interlevel spacing and that the relaxation by emission of acoustic phonons, though possible for all energy level spacings, is very slow<sup>1-3</sup>. Most experimental results contradict this prediction.

The alternative mechanism is fast relaxation

due to carrier-carrier collisions<sup>4,6</sup>. This mechanism is assumed to be efficient when several carriers are present in the QD. If only one electron-hole pair is present in the QD, the final step of the relaxation should be again phonon assisted relaxation of at least one of the carriers.

We consider here both mechanisms of the carrier relaxation. In particular, we discuss the experimental conditions when one or another of the mechanisms is responsible for the carrier relaxation.

## II. PHONON-ASSISTED CARRIER RELAXATION

The carrier relaxation with emission of phonons determines the lower limit of the relaxation rate because of weak carrier-phonon interaction. Therefore this process can be observed when there is only one hot carrier in QD. Generally a three steps of relaxation

should be considered. The first one is the carrier capture from a barrier layer into the QD if the carrier is created by light absorption in barrier layer or by electric current through the heterostructure. This capture is studied in several papers, see, for example, Refs.<sup>7,8</sup> and references therein.

The second step of the carrier relaxation is a cascade relaxation over discrete energy levels of a QD. A rate of this relaxation depends on the interlevel spacings and on phonon spectrum of a QD. Generally different relaxation channels through the different intermediate states, including the mixed electron-phonon states are possible to reach the lowest energy state. This complicated process is still not studied in detail<sup>9</sup>.

As the third step of relaxation, we separate out the final relaxation of the carrier from the first excited state to its ground state. On the one hand, usually this is the slowest step of relaxation which mostly determines the relaxation rate. On the other hand, we developed the experimental technique which allows us to study this step of relaxation separately<sup>10,11</sup>.

We studied heterostructures with InP and InGaAs self-assembled quantum dots. Photoluminescence (PL) of the samples was excited selectively within the PL band of QD's. So the excitation created an electron and a hole in their ground or first excited states. And we can study in this case only the last step of the relaxation. We used two different methods for this study.

At first, we measured PL spectra of the samples in presence of external electric field.

The examples of the PL spectra for the InP and InGaAs QD's are shown in Figs. 1 and 2, respectively. As seen, the integral PL intensity decreases when a negative bias is applied to the sample surface.

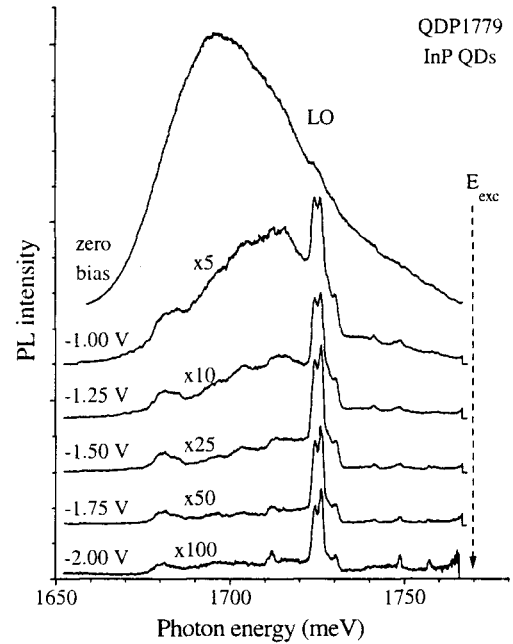


FIG. 1. PL spectra of InP QD's at various applied bias. The spectral position of the excitation is marked by an arrow. The most intense resonance shifted from the laser line by the LO phonon energy is marked as LO. The applied bias is shown near each spectrum. For clarity, the curves are scaled and shifted vertically.

At the same time, the decrease of the PL in different spectral points is different and, as a result, pronounced resonances appear in the PL spectra. The most prominent resonance in the spectra of the InP QD's is shifted from the excitation line approximately by the LO phonon energy of the bulk InP crystal ( $\hbar \omega_{LO} = 43.5$  meV).

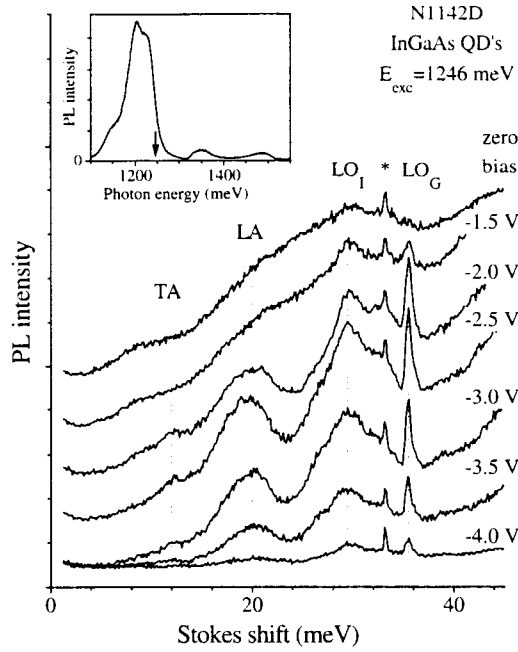


FIG.2. The PL intensity versus Stokes shift for the sample N1142D with InGaAs QD's under different biases indicated near each curve and  $E_{exc} = 1246$  meV. The spectra are shifted vertically for clarity. The energies of the resonances marked by TA, LA,  $LO_1$ , and  $LO_G$  are 12 meV, 20 meV, 30 meV, and 35.5 meV, respectively. Inset: PL spectrum of the sample without bias.

In the case of the InGaAs QD's, the most prominent resonances can be assigned to the GaAs-like and InAs-like LO phonons of the InGaAs QD's because their energy shifts from the excitation line are close to the energy of the LO phonons in GaAs and InAs crystals, respectively. They are marked in Fig. 2 as  $LO_G$  and  $LO_1$ . The intense resonance with a Stokes shift of about 20 meV can be assigned to the longitudinal acoustic (LA) phonons of InGaAs solid solution. A narrow peak with a Stokes shift of 33.2 meV marked by "\*" in

Fig.2 is probably caused by the Raman scattering from the GaAs substrate because the intensity of this peak does not depend on bias.

The phonon resonances are caused by the selective phonon-assisted relaxation of hot carriers in the presence of nonradiative losses. Appearance of the phonon resonances due to this process can be explained as follows<sup>12-14</sup>. The quasiresonant excitation creates electrons and holes in the excited states. The QD's in the ensemble have slightly different sizes and shapes, and the interlevel energy spacing,  $\Delta E$ , has some distribution. The spacing  $\Delta E$  can well match the LO phonon energy,  $E_{LO}$ , only in some subset of the QD's. Carrier relaxation in these QD's is fast due to high efficiency of this process with emission of an LO phonon. The relaxation in the rest of the QD's occurs via emission of acoustic phonons i.e., via a much slower process. If the electron or hole can effectively leave the QD (this process is usually referred to as nonradiative losses) before relaxation via the acoustic phonon emission, the PL does not appear in any spectral point except the point where it is "saved" by the fast LO-phonon assisted relaxation. In the time-integrated PL spectrum, a narrow peak shifted from the excitation line by the energy of the LO phonon,  $E_{LO}$ , must be observed in this case. However, if there are no significant nonradiative losses, electrons and holes in any QD eventually relax to the lowest levels and recombine. In this case, the PL spectrum must reproduce the energy distribution of the lowest optical transition that usually has a bell-like smooth shape. Behavior of the

spectra presented in Figs. 1, 2 agrees with this scenario.

The main process of nonradiative losses activated by the external electric field is the tunneling of the photocreated carriers from the QD into the barrier layer<sup>15</sup>. The electric field changes the potential profile so that it acquires a triangular shape. A width of the potential barrier depends on electric field. This width and, as a result, the tunneling rate can be changed artificially by changing of applied bias. This opens up a wide possibility for comparative study in steady state conditions of the relaxation process with emission of different type of phonons.

The intense LO phonon resonances seen in Figs. 1, 2 argue for the fast LO-phonon-assisted relaxation. This is a well known result. An interesting and new feature is that the PL spectra of the biased samples reveal many acoustic phonon resonances<sup>15,16</sup>. In Fig. 3 we plotted the PL spectra measured at different photon energies of excitation. It is seen that the acoustic phonon resonances are clearly observed not only between the laser line and the 1LO resonance but also between the 1LO and 2LO resonances. Their energy shifts coincide with the energy of the high frequency transverse acoustic (TA) and LA phonons in bulk InP crystal. A small peak at 30 meV marked by LA<sub>b</sub> can be assigned to LA phonons of InGaP barrier. This observation argues for a rather efficient relaxation with emission of the high frequency acoustic phonons. So efficient relaxation is in stark contrast with the theoretical predictions<sup>1,3</sup>.

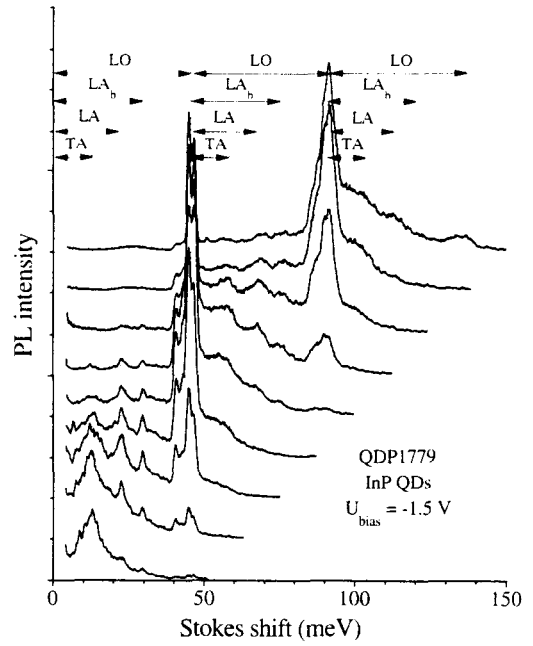


FIG. 3. The PL spectra at different photon energies of excitation (from top to bottom) versus Stokes shift.  $U_{\text{bias}} = -1.5$  V. The spectra are shifted vertically for clarity. Similar phonon resonances in different spectra are marked by dashed lines. The arrows labelled TA etc. indicate the energy shift of the resonances from the laser line or 1LO or 2LO resonances.

To support our observation of the acoustic-phonon-assisted relaxation, we performed the PL kinetics measurements. They were done using a picosecond Ti:sapphire laser with a pulse duration ranging from 1 to 5 ps and a repetition rate of 82 MHz. A 0.25 m double subtractive dispersion monochromator (spectral resolution 0.5 nm) and a streak camera were used for accumulation of the signal in the selected spectral points. The time resolution of the setup was about 6 ps.

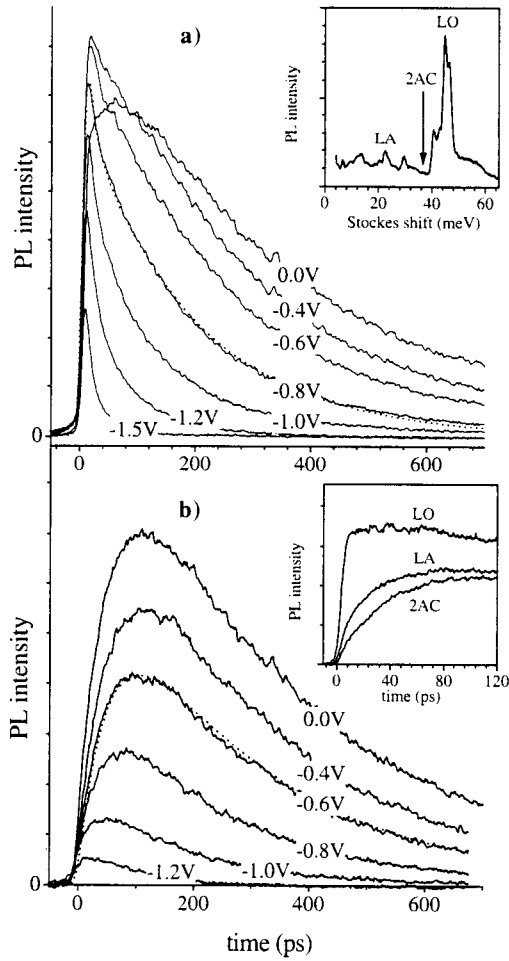


FIG. 4. PL kinetics at the LO (a) and 2AC (b) spectral points (marked in the upper inset) for different biases indicated near each curve. Examples of fits of the LO kinetics at  $U_{\text{bias}} = -0.8\text{V}$  and the 2AC kinetics at  $U_{\text{bias}} = -0.6\text{V}$  by the Eq.(1) are shown by dotted lines. Upper inset: PL spectrum at  $U_{\text{bias}} = -1.5\text{V}$ . Lower inset: initial part of the PL kinetics at zero bias for a few spectral points marked in the upper inset.

The PL kinetics for a few spectral points within the PL band under quasiresonant excitation are shown in Fig. 4. At zero bias, the kinetics consists of a short rising part and a rather long decay. The PL leading edge is

shorter than the time resolution of the setup for LO resonance and much longer for other spectral points as is shown in the inset. At negative bias, the decay becomes faster and the amplitude of the signal becomes smaller. This behavior of the PL kinetics is clearly understood. At zero bias, the PL decay is most probably determined by the radiative recombination of the electron-hole pair. When the negative bias is applied, the PL decay shortening is caused by the nonradiative losses of excitation due to tunneling of the holes from the QD's. The PL rise is controlled by the carrier relaxation. The whole time evolution of the PL intensity is well described by simple equation

$$I_{\text{PL}}(t) = I_0 (e^{-t/\tau_{\text{PL}}} - e^{-t/\tau_r}) \quad (1)$$

where  $\tau_{\text{PL}}$  is the PL decay time and  $\tau_r$  is the relaxation time of hot carriers.

We measured the PL kinetics of the sample with the InP Qd's in many spectral points and determined the spectral dependence of the relaxation rate  $\gamma_r = \tau_r^{-1}$ . It is shown in Fig. 5. The relaxation rate shows a very prominent spectral dependence with distinct phonon resonances. According to the above discussion, these are caused by the relaxation of the hot carriers with emission of TA, LA or LO phonons. An interesting new feature is the fast carrier relaxation with emission of the acoustic phonons with small enough energy of a few meV (denoted by FA in Fig. 5). We believe that this is an experimental evidence of the theoretically proposed enhanced interaction with phonons whose wavelengths match the QD size<sup>1,3</sup>.

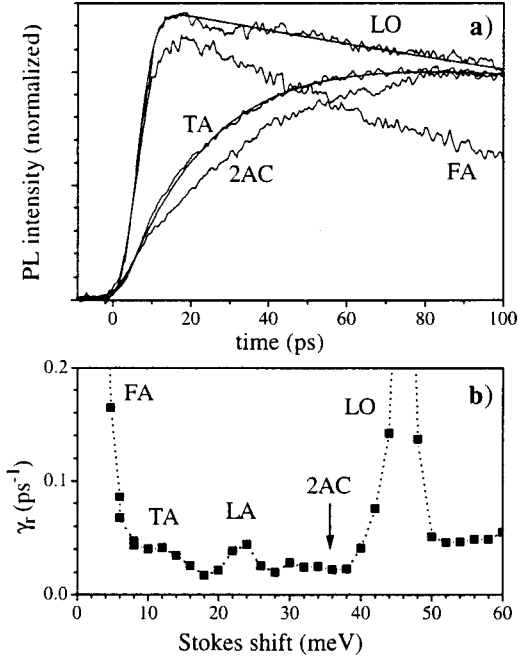


FIG. 5. (a) PL kinetics of the sample QDP1778 at  $U_{bias} = -0.8$  V for several spectral points indicated in (b) (noisy curves). The fit by the function (1) is shown by the smooth curves. (b) The relaxation rate versus Stokes shift. The dotted line is a guide to the eye.

The presented experimental data clearly show that the interaction of the carriers with acoustic phonons is stronger than that predicted theoretically by the orders of magnitude and is able to cause an efficient carrier relaxation within a few tens of picoseconds. The interaction with the high energy acoustic phonons may be enhanced for a few reasons. The first one is the small group velocity of the phonons that lengthens the interaction time. The second one is the piezoelectric effect in these crystals that leads to long range electric fields associated with acoustic phonons. Finally, the interaction with phonons of large momentum may be

enhanced due to  $\Gamma$  - X - L valley mixing in QD's. To construct an adequate model, it is necessary to go beyond the widely used effective mass approximation. At the present stage, modelling of the electron-hole-phonon interaction at large phonon wave vector  $q$  is an open theoretical problem.

### III. CARRIER-CARRIER SCATTERING

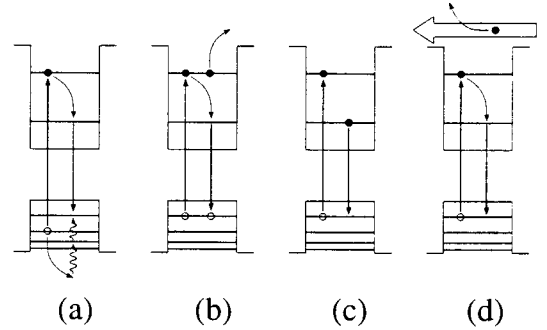


FIG. 6. Different Auger-like processes causing fast carrier relaxation. (a) electron-hole scattering, (b) carrier-carrier scattering in presence of two electron-hole pair, (c) relaxation in a charged QD, and (d) electric-current induced relaxation.

The phonon-assisted relaxation can be observed only under specific experimental conditions. Carrier-carrier scattering usually referred to as Auger process can considerably accelerate the relaxation<sup>4-6</sup>. Relaxation due to Auger process must be fast because the carriers as charged particles interact with each other much stronger than with phonons. We consider here a few particular processes illustrated schematically in Fig 6. To simplify our discussion, we assume that an excitation creates an electron in the excited state and a

hole in the ground state. We can partially justify this assumption for the biased sample because selection rules for optical transitions are broken in this case.

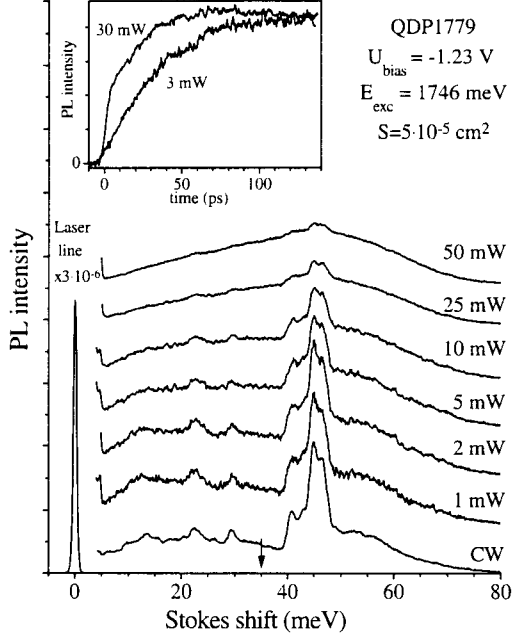


FIG. 7. PL spectra of the biased sample QDP1779 with InP QD's under CW excitation (bottom curve) and pulsed excitation with power indicated near each curve. The laser spot area on the sample is  $S = 5 \times 10^{-5} \text{ cm}^2$ , photon energy of the excitation  $E_{\text{exc}} = 1746 \text{ meV}$  and electric bias  $U_{\text{bias}} = -1.23 \text{ V}$ . An arrow marks the 2AC spectral point where the PL kinetics was measured. Inset: the initial part of the PL kinetics under various excitation powers indicated.

The simplest process is the electron hole scattering drawn in Fig. 6a. In this process, an excess energy of the hot electron is transferred to the hole. As a result, the electron goes down to its ground state and the hole is excited up to some high energy level. Then the hole relaxes with emission of

phonons. This process is assumed to be faster than the phonon-assisted relaxation of the electron because the interlevel spacing for holes in QD's is usually considerably less than that for electrons. Of course, energy spacing between some hole states must well match the interlevel spacing for electron to fulfill the energy conservation rule. This condition is easily fulfilled for InP QD's due to shallow potential well for hole that results in high density of the excited hole states. For many other QD's, the energy structure is not so precisely known to determine uniquely whether this process may occur or not. This process is usually difficult to recognize in optical experiment because both carriers, an electron and a hole, are always present in the QD and can be scattered by each other independent on experimental conditions.

Next process (Fig. 6b) occurs when the excitation creates more than one electron hole pairs. In this case, any carrier can loose its excess energy and one of the others acquires it if the energy conservation rule is fulfilled. It is evident that the efficiency of this process must depend on the number of carriers in the QD because each carrier can be scattered by any other one. In the simplest model, the dependence on the pump power should be quadratic. We can illustrate this process by the PL spectra of the biased sample detected at different power densities of excitation (Fig. 7). As seen, the acoustic phonon resonances disappear and the LO resonance becomes barely observable under strong pumping. This fact means that the relaxation rate for all interlevel spacings becomes comparable to

the LO phonon-assisted relaxation rate. The PL kinetics reveals a shortening of the PL rise time with increase of the pumping (see inset in Fig. 7) which also indicates acceleration of the carrier relaxation.

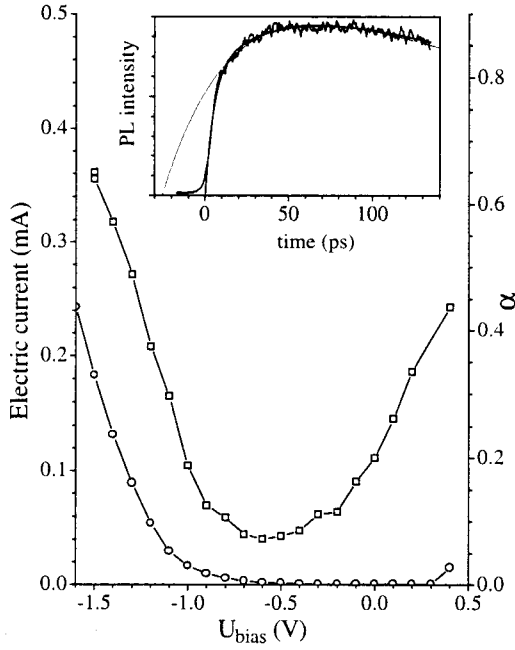


FIG. 8. Bias dependence of the step in the PL rise at LA resonance (squares) and of electric current (circles) for sample QDP1779. Inset: PL kinetics at zero bias (noisy curve) and the fit of only the slow PL rise (dashed curve). The abrupt PL rise is clearly seen.

Third process (Fig. 6c) is caused by charging of QD's. At positive bias, electrons can be moved from n-doped substrate to the QD's which are deep potential wells for the electrons. Dynamics of the whole system, a cold electron and a hot photocreated electron-hole pair, is complicated and can be mostly controlled by carrier-carrier scattering. Spectral dependence of the relaxation rate does not contain in this case any phonon resonances. A bias dependence reveals a

gradual increase of the abrupt PL rise with the increase of bias as shown in Fig. 8. This abrupt PL rise is probably caused by recombination of cold electron transferred from substrate with the photocreated cold hole. Strictly speaking, the fast PL rise does not relate in this particular case to any relaxation process therefore the step in the PL rise merely reflects a probability of the QD precharging.

Last process (Fig 6d) is the electric-current-induced relaxation. The flowing carriers can interact with the carriers inside QD's and cause their relaxation. We can illustrate this process by the bias dependence of the abrupt PL rise at strong enough negative bias when no other Auger processes were involved (Fig. 8). As seen the fast PL rise portion increases with increase of electric current through the sample.

#### IV. CONCLUSION

We discussed several relaxation processes. Each of them occurs in some special experimental conditions. The phonon-assisted relaxation occurs at low power density of excitation when only one electron-hole pair is created in a QD. The relaxation time is very fast when interlevel energy spacing coincides with the LO phonon energy. It is much longer for the acoustic-phonon-assisted relaxation. But it is not so long as predicted theoretically, only of about few or several tens of picoseconds. High density of excitation, or charging of QD's, or electric current can drastically accelerate the relaxation due to



carrier-carrier interaction. We illustrated a discussion of each particular process by relevant experimental data.

---

<sup>1</sup> U. Bockelmann and G. Bastard, *Phys. Rev. B* **42**, 8947 (1990).

<sup>2</sup> H. Benisty, C. M. Sotomayor-Torrès, and C. Weisbuch, *Phys. Rev. B* **44**, 10945 (1991).

<sup>3</sup> T. Inoshita and H. Sakaki, *Phys. Rev. B* **46**, 7260 (1992).

<sup>4</sup> U. Bockelmann and T. Egeler, *Phys. Rev. B* **46**, 15574 (1992).

<sup>5</sup> A. L. Efros, V. A. Kharchenko, and M. Rosen, *Solid State Commun.* **93**, 281 (1995).

<sup>6</sup> S. Nair and Y. Masumoto, *J. Lumin.* **87-89**, 408 (2000) *Phys. Status Solidi (b)* **178**, 303 (2000).

<sup>7</sup> B. Ohnesorge, M. Albrecht, J. Oshinowo, A. Forchel, and Y. Arakawa, *Phys. Rev. B* **54**, 11532 (1996).

<sup>8</sup> S. Raymond, K. Hinzer, S. Fafard, and J. L. Merz, *Phys. Rev. B* **61**, R16331 (2000).

<sup>9</sup> S. Raymond, X. Guo, J. L. Merz, and S. Fafard, *Phys. Rev. B* **59**, 7624 (1999).

<sup>10</sup> I. E. Kozin, I. V. Ignatiev, H.-W. Ren, S. Sugou, and Y. Masumoto, *J. Lumin.* **87-89**, 441 (2000).

<sup>11</sup> I. V. Ignatiev, I. E. Kozin, S. V. Nair, H.-W. Ren, S. Sugou, and Y. Masumoto, *Phys. Rev. B* **61**, 15633 (2000).

<sup>12</sup> S. Fafard, R. Leon, D. Leonard, J. L. Merz, and P. M. Petroff, *Phys. Rev.*

*B* **52**, 5752 (1995).

<sup>13</sup> R. Heitz, M. Grundmann, N. N. Ledentsov, L. Eckey, M. Veit, D. Bimberg, V. M. Ustinov, A. Yu. Egorov, A. E. Zhukov, P. S. Kop'ev, and Zh. I. Alferov, *Appl. Phys. Lett.* **68**, 361 (1996).

<sup>14</sup> K. H. Schmidt, G. Medeiros-Ribeiro, M. Oestreich, P. M. Petroff, and G. H. Döhler, *Phys. Rev. B* **54**, 11346 (1996).

<sup>15</sup> I. V. Ignatiev, I. E. Kozin, V. G. Davydov, S. V. Nair, J. S. Lee, H. W. Ren, S. Sugou, and Y. Masumoto, *submitted to Phys. Rev. B*

<sup>16</sup> V. G. Davydov, I. V. Ignatiev, I. E. Kozin, S. V. Nair, J. S. Lee, H. W. Ren, S. Sugou, and Y. Masumoto, *submitted to Phys. stat. sol.(b)*